

# Interaction of tetraethoxysilane with OH-terminated SiO<sub>2</sub> (0 0 1) surface: A first principles study



Xiaodi Deng<sup>a,\*</sup>, Yixu Song<sup>b,\*\*</sup>, Jinchun Li<sup>c</sup>, Yikang Pu<sup>a</sup>

<sup>a</sup> Department of Engineering Physics, Tsinghua University, Beijing 100084, People's Republic of China

<sup>b</sup> State Key Laboratory on Intelligent Technology and Systems, Tsinghua National Laboratory for Information Science and Technology, Department of Computer Science and Technology, Tsinghua University, Beijing 100084, People's Republic of China

<sup>c</sup> Institute of Applied Physics, University of Science and Technology Beijing, Beijing 100083, People's Republic of China

## ARTICLE INFO

### Article history:

Received 14 January 2014

Received in revised form 4 March 2014

Accepted 7 March 2014

Available online 15 March 2014

### Keywords:

Tetraethoxysilane

SiO<sub>2</sub>

Atomic layer deposition

Reaction barrier

Surface reaction

First principle

## ABSTRACT

First principles calculations have been performed to investigate the surface reaction mechanism of tetraethoxysilane (TEOS) with fully hydroxylated SiO<sub>2</sub>(0 0 1) substrate. In semiconductor industry, this is the key step to understand and control the SiO<sub>2</sub> film growth in chemical vapor deposition (CVD) and atomic layer deposition (ALD) processes. During the calculation, we proposed a model which breaks the surface dissociative chemisorption into two steps and we calculated the activation barriers and thermochemical energies for each step. Our calculation result for step one shows that the first half reaction is thermodynamically favorable. For the second half reaction, we systematically studied the two potential reaction pathways. The comparing result indicates that the pathway which is more energetically favorable will lead to formation of crystalline SiO<sub>2</sub> films while the other will lead to formation of disordered SiO<sub>2</sub> films.

© 2014 Elsevier B.V. All rights reserved.

## 1. Introduction

Tetraethoxysilane (TEOS) has been widely used to deposit silicon dioxide in chemical vapor deposition (CVD) [1] and plasma enhanced chemical vapor deposition (PECVD) [2] since a long time. As the demands of reducing the sizes of devices in semiconductor industry continues, atomic layer deposition (ALD) technique [3–5] is used to grow conformal thin films that are in precision of monolayer. ALD deposition of SiO<sub>2</sub> thin film with TEOS and oxidizing gas has been reported by Ferguson et al. [6]. ALD involves cycles of precursor self-limiting adsorption on substrate and reactivation of the surface. Therefore, to control the SiO<sub>2</sub> ALD film deposition with TEOS at atomic precision, we must understand the surface reaction mechanism of TEOS with the substrate surfaces. However, to our acknowledgment very few studies have been addressed on this subject. For TEOS surface chemisorption reactions, several models have been proposed. Coltrin et al. build a serial of surface reaction models that a TEOS molecule will firstly reacts with the surface OH

and release an ethanol, then the adsorbed species on the surface will undergo self-decomposing with releasing of ethylene gases and formation of new OH terminals [7]. The ALD reaction model proposed by Ferguson et al. has very similar process for the first step reaction while they believed that the formation of new OH functional groups is the results of the adsorbed species reacting with oxidizing gases such as H<sub>2</sub>O and NH<sub>3</sub> [6]. On the other hand, however, Sato et al. proposed a completely different model recently that TEOS can not directly adsorb to the surface Si–OH [8] because TEOS does not have any polarity [9]. All these models show that reaction mechanism of TEOS surface reactions are still not fully understood. In this study, we performed first principles calculations to investigate the reaction mechanism of TEOS with fully hydroxylated SiO<sub>2</sub> (0 0 1) surface. Here, our interest is mainly focused on the TEOS adsorption behavior at the early stage of SiO<sub>2</sub> ALD deposition as it is the key step to control the quality of the deposited film. We believe that with fully understanding of this step will enable us to design better processes to deposit more conformal, higher purity SiO<sub>2</sub> films.

## 2. Computational method

All calculations were performed based on the density functional theory (DFT) with the PW91 [10,11] version of the generalized gradient approximation (GGA) for the exchange–correlation functional

\* Corresponding author. Tel.: +86 13501263438.

\*\* Corresponding author.

E-mail addresses: [dixiaodeng@gmail.com](mailto:dixiaodeng@gmail.com) (X. Deng), [songyixu@163.com](mailto:songyixu@163.com) (Y. Song).

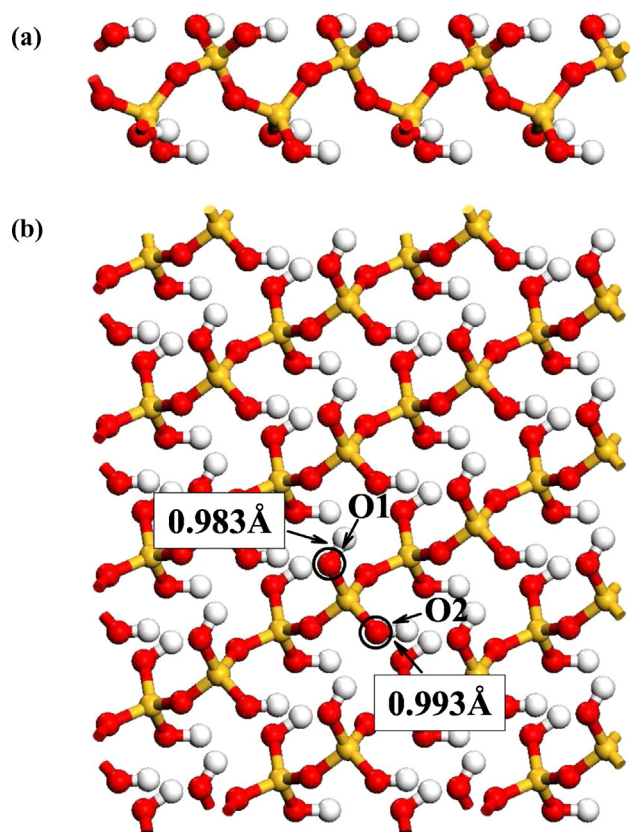


Fig. 1. Optimized surface structure of hydroxylated  $\text{SiO}_2(001)$ : (a) side view; (b) top view.

which have been implemented in Vienna ab initio simulation package (VASP) [12,13]. The cutoff energy for plane wave basis is set to 550 eV and the Brillouin zone integration was sampled within a  $2 \times 2 \times 1$  k-point mesh using Monkhorst–Pack method [14]. Structure optimization was performed to make sure that the force on each atom is less than 0.05 eV/Å. Transition-state structure search and barrier energy calculation were carried out using the climbing nudged elastic band (CNEB) tool [15,16].

A seven-layer  $\text{SiO}_2(001)-(4 \times 4)$  slab was modeled with the surface fully hydroxylated. The top view and side view of the substrate model are shown in Fig. 1. The supercell contains 32 Si atoms, 96 O atoms and 64 H atoms, with a total number of 192 atoms. In addition to the TEOS molecule, there are about 225 atoms in the system during the calculations. A vacuum thickness of 12 Å is used to separate adjacent slabs. The bottom two O layers and a Si layer are fixed during structure optimization. The optimized surface geometry and structure parameters are agree with DFT calculations of previous reports [17,18]. To analyze the electrostatic property of TEOS molecule, DFT calculations with the same exchange-correlation functional are performed using DMol<sup>3</sup> package [19,20]. The optimized structure and electrostatic potential of TEOS molecule are shown in Fig. 2. The structure parameters are almost identical with the results reported by Phadungsukanan et al. [21].

### 3. Results and discussion

TEOS has four ethoxy functional groups. From the electrostatic potential shown in Fig. 2, we can clearly see that positive charges are mostly concentrated on Si atoms and H atoms and negative charges are on O atoms. When TEOS is approaching the surface there will be strong attractions between O atoms and surface H atoms. At the same time the positive charged Si atom will attack surface O

Table 1

Main optimized bond lengths of the initial state (IS), transition state (TS) and final state (FS) for the first step reaction.

Distances	IS	TS	FS
$\text{Si}^p\text{—O}^p$	1.672	1.863	3.640
$\text{Si}^p\text{—O}^s$	3.991	2.386	1.616
$\text{O}^p\text{—H}^s$	1.687	1.022	3.460
$\text{O}^s\text{—H}^s$	1.003	1.566	0.979

atom. As a consequence, bonds broken are most likely to happen between the Si—O bond. Therefore, TEOS absorption on the surface is an ethoxy functional group removal process.

The chemisorption and deposition of TEOS on OH-terminated  $\text{SiO}_2$  surface can be broken into two steps. In the first step, TEOS chemisorbs on the surface and releases an ethane. In the second step, another ethoxy branches of TEOS reacts with OH on the surface and release a second ethane. The reaction process of these steps are illustrated in Fig. 3.

As shown in Fig. 1 there are two types of O—H groups on the substrate surface. The one labeled with O1 has bond length of 0.983 Å while the one labeled with O2 has longer bond length of 0.993 Å. As pointed out by Li et al. [18], the O1 type of O—H group is more accessible for electrophilic attacks by gas phase precursors. Therefore, in our calculations, we chose O1 type O—H as the TEOS adsorption site for the first step reaction. Here, we calculated the energy profile along the prescribed pathway. The optimized structures of initial state (IS), transition state (TS) and final state (FS) are shown in Fig. 4, the parameters of these optimized structures are listed in Table 1. At the initial stage of step one, TEOS is adsorbed on the  $\text{SiO}_2$  surface through strong hydrogen bond between O atom of one of the TEOS branch ( $\text{O}^p$ ) and H atom of the hydroxyl group ( $\text{H}^s$ ) on the  $\text{SiO}_2$  surface. This strong bond attraction results in a small deformation of the surface H configuration. Comparing with other surface O—H bonds, there is about 90° orientation change of the affected surface  $\text{O}^p\text{—H}^s$  bond. It changes from horizontally orientated to almost vertically orientated. The bond length of  $\text{O}^p\text{—H}^s$  also changes from 0.984 Å to 1.003 Å during the surface deformation. The surface H movement clearly shows the fact that the attraction of the TEOS ethoxy functional groups ( $\text{OCH}_2\text{CH}_3$ ) is higher than that of the surface O atoms. When the TEOS molecule continue approaching to the surface, H atom migrates from surface O atom ( $\text{O}^s$ ) to O atom in the TEOS ethoxy functional group ( $\text{O}^p$ ). Simultaneously, Si atom in the TEOS ( $\text{Si}^p$ ) contacts to the surface O atom ( $\text{O}^s$ ). In the transition state of this surface adsorption step,  $\text{O}^p\text{—H}^s$  bond is elongated while weak  $\text{Si}^p\text{—O}^s$  and  $\text{O}^p\text{—H}^s$  bonds are formed. The  $\text{O}^s\text{—H}^s$  bond length increases from 0.984 Å to 1.566 Å and  $\text{O}^p\text{—H}^s$  bond length decreases from 1.687 Å to 1.022 Å. The increment of  $\text{Si}^p\text{—O}^p$  distance from 1.672 Å to 1.863 Å clearly shows the dissociation of TEOS ethoxy functional group. As the reaction goes on, the  $\text{Si}^p\text{—O}^p$  bond will be completely broken. A very stable Si—O bond will be formed between Si in TEOS and the surface O atom with a bond length of about 1.616 Å. As a consequence, in the final state of this reaction step ( $\text{C}_2\text{H}_5\text{O})_3\text{Si}$  species are adsorbed on the surface and an ethanol is released into the gas phase. Fig. 5 shows the calculated energy profile. The reaction energy of this step is −3.1 kcal/mol which means that this reaction process is thermodynamically favorable. The reaction barrier of this step is 48.3 kcal/mol.

After the first step reaction,  $(\text{C}_2\text{H}_5\text{O})_3\text{Si}$  species is adsorbed on the  $\text{SiO}_2(001)$  surface. In Fig. 6 we marked the three possible attacking sites for the second ethoxy branch as  $\text{S2}_a$ ,  $\text{S2}_b$  and  $\text{S2}_c$ . However, after further analyzing the surface geometry of the first step reaction, we noticed that the two surface O—H bonds at site  $\text{S2}_a$  and  $\text{S2}_b$  reoriented themselves towards to the corresponding nearby O atoms on the adsorbed  $(\text{C}_2\text{H}_5\text{O})_3\text{Si}$  ethoxy branches. With a reasonable assumption that the attractions between the surface

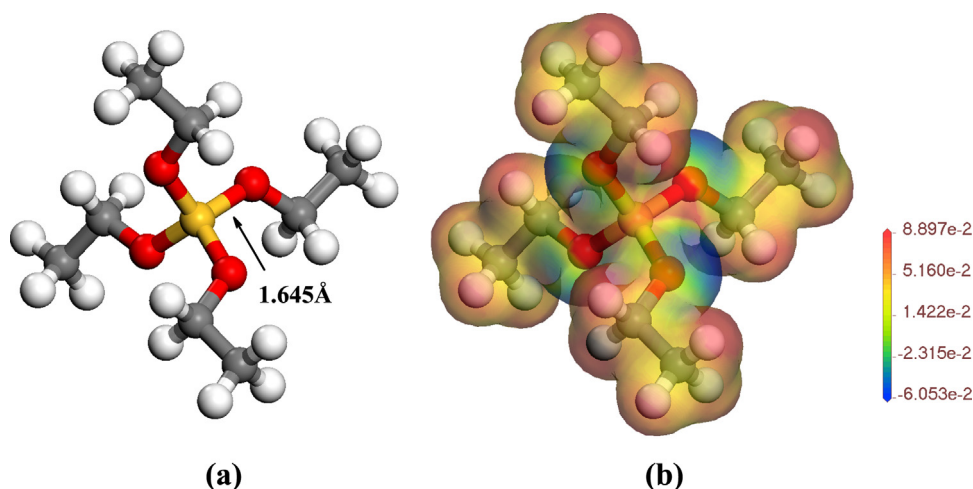


Fig. 2. TEOS molecule: (a) the optimized structure; (b) the calculated electrostatic potential.

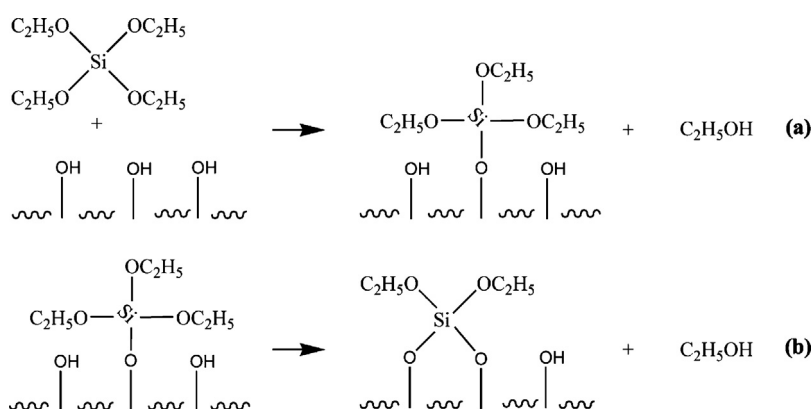


Fig. 3. Proposed reaction model: (a) the first step reaction; (b) the second step reaction.

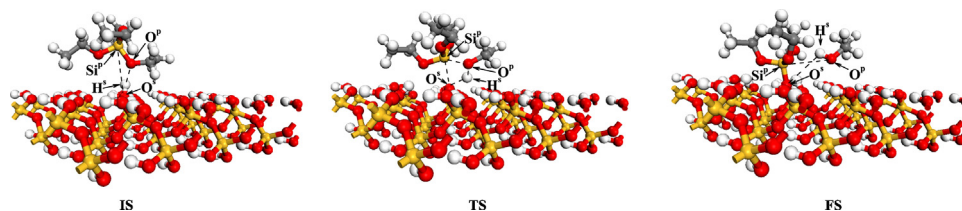


Fig. 4. The optimized structure of the initial state (IS), transition state (TS) and final state (FS) for the first step reaction.

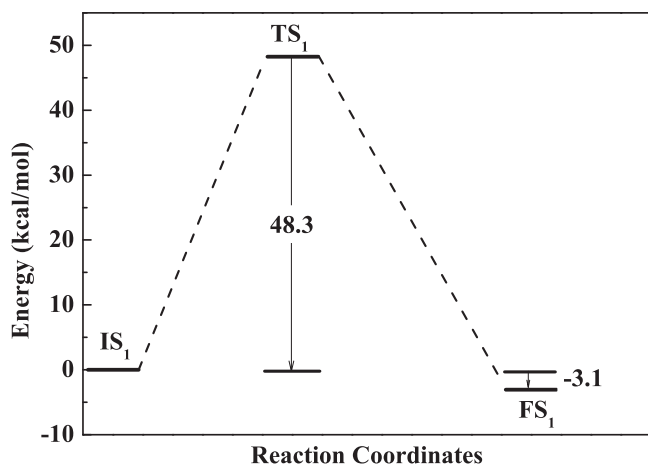


Fig. 5. The calculated energy profile for the first step reaction.

O—H group and each of the three ethoxy branches in the adsorbed  $(\text{C}_2\text{H}_5\text{O})_3\text{Si}$  species are equal, the attraction of site  $\text{S2}_c$  will be outweighed by the attractions of site  $\text{S2}_a$  and  $\text{S2}_b$ . This makes reactions at site  $\text{S2}_c$  are almost impossible to happen. Therefore, in our calculations, reactions at only site  $\text{S2}_a$  and  $\text{S2}_b$  were considered. These two reaction sites correspond to two possible dissociative sites for another ethoxy fragment in the adsorbed species. In Fig. 6, the pathways at site  $\text{S2}_a$  and  $\text{S2}_b$  are marked as path-a and path-b, respectively. All these reaction pathways will form O—Si—O bridge like structure on the surface.

For the first possible reaction pathway (path-a), the optimized initial state, transition state and final state are shown in Fig. 7, the main bond lengths during the reaction are listed in Table 2. In the initial state the ethoxy function group around site  $a$  ( $\text{S2}_a$ ) attracts the nearby surface O—H. A very obvious reorientation of the O—H has been observed. The reorientation angle is as large as  $120^\circ$ . Atomic configuration of Si in the  $(\text{C}_2\text{H}_5\text{O})_3\text{Si}$  species ( $\text{Si}^p$ ), O in the ethoxy function group ( $\text{O}^p$ ), surface O ( $\text{O}^s$ ) and surface

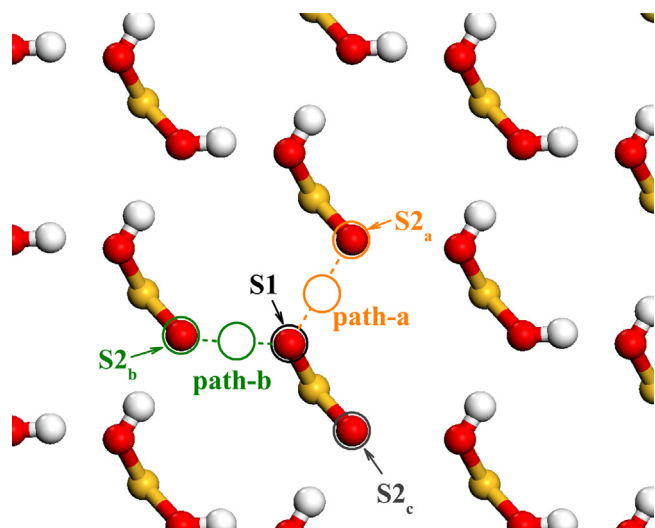


Fig. 6. Two possible reaction pathways for the second step reaction.

Table 2

Main optimized bond lengths of the initial state (IS), transition state (TS) and final state (FS) for the second step reaction path-a.

Distances	IS	TS	FS
Si <sup>p</sup> —O <sup>p</sup>	1.635	1.821	3.616
Si <sup>p</sup> —O <sup>s</sup>	3.809	2.203	1.662
O <sup>p</sup> —H <sup>s</sup>	1.664	1.158	0.972
O <sup>s</sup> —H <sup>s</sup>	0.995	1.255	3.185

H (H<sup>s</sup>) undergoes subtle changes when the reaction goes into the transition state. Weak bond connections are formed among these four atoms. The bond lengths of Si<sup>p</sup>—O<sup>p</sup> and Si<sup>p</sup>—O<sup>s</sup> are 1.821 Å and 2.203 Å, respectively. The bond lengths of O<sup>p</sup>—H<sup>s</sup> and O<sup>s</sup>—H<sup>s</sup> are 1.158 Å and 1.255 Å, respectively. They are all longer than the normal Si—O and O—H bond lengths. No stable bonds form during this stage. This unstable state will not last very long before it transits into the final state with releasing of an ethanol into the gas phase and formation of stable O—Si—O bridge structure on the SiO<sub>2</sub> surface. The bond angle of the newly formed O—Si—O bridge structure is 111.4° and it is almost identical to that of the SiO<sub>2</sub> substrate which is 107.6°. This process is not thermodynamically favorable and the reaction energy is about 6.4 kcal/mol.

Table 3

Main optimized bond lengths of the initial state (IS), transition state (TS) and final state (FS) for the second step reaction path-b.

Distances	IS	TS	FS
Si <sup>p</sup> —O <sup>p</sup>	1.647	1.835	3.981
Si <sup>p</sup> —O <sup>s</sup>	3.626	2.280	1.629
O <sup>p</sup> —H <sup>s</sup>	1.708	1.056	0.973
O <sup>s</sup> —H <sup>s</sup>	0.994	1.443	4.045

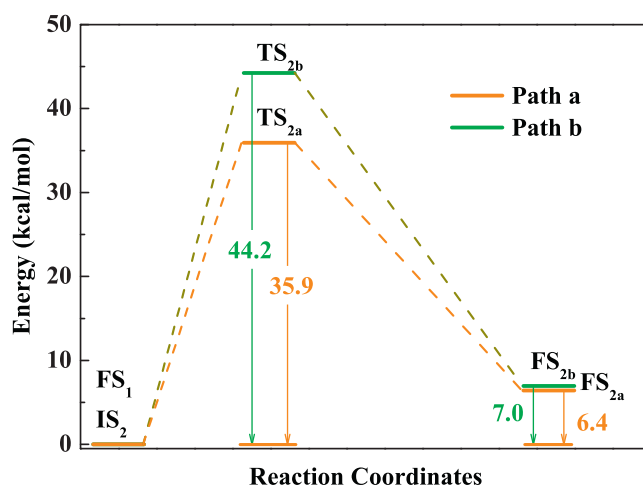


Fig. 9. Comparing of the energy profiles of the second step reaction along path-a and path-b.

The calculated initial state, transition state and final state of the second possible pathway (path-b) are shown in Fig. 8 and the corresponding structure parameters are listed in Table 3. The reaction process of this pathway is quite similar with reaction pathway path-a. However, the Si<sup>p</sup>—O<sup>s</sup> distance (2.280 Å) at the transition state is longer than that of path-a (2.203 Å). This indicates that the Si—O bond formation for path-b is harder than path-a. Indeed, the calculated reaction energy barrier for path-b (44.2 kcal/mol) is much higher than that of path-a (35.9 kcal/mol). The bond angle of the bridge O—Si—O structure in the final state is 110.268°.

Comparing of the reaction energy profile with path-a and path-b is illustrated in Fig. 9. The structure geometry of the final state for both pathways is very similar to each other and the O—Si—O bond angles are very close to 109° which is typical angle for sp<sup>3</sup> hybridization. Therefore, the reaction energies for path-a and

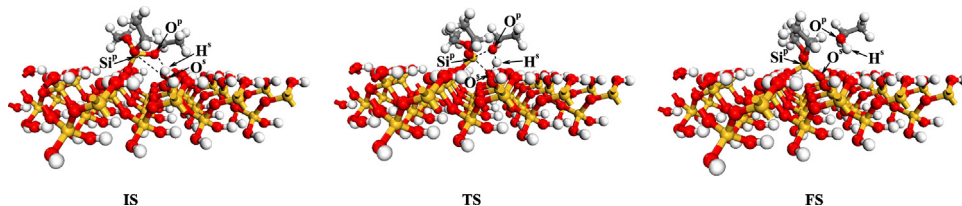


Fig. 7. The optimized structure of the initial state (IS), transition state (TS) and final state (FS) for the second step reaction along path-a.

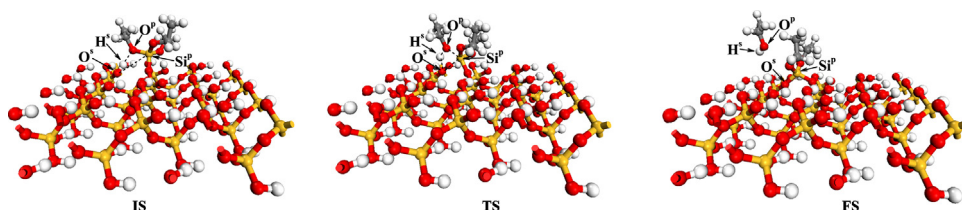


Fig. 8. The optimized structure of the initial state (IS), transition state (TS) and final state (FS) for the second step reaction along path-b.



path-b are almost identical. The energy difference between path-a and path-b is only 0.6 kcal/mol and path-a is slightly more thermodynamically favorable. Furthermore, the activation barrier for path-a is also much lower than path-b. Consequently, removal of the second ethoxy functional group of TEOS is more likely to happen along path-a. The conclusion is quite obvious when we study much closer to the final structure of path-a and path-b. The orientation of the O–Si–O bridge structure for path-a is the same to SiO<sub>2</sub> (001) crystalline arrangement while for path-b it is in the opposite direction. As a result, crystalline SiO<sub>2</sub> film will be formed if the reactions go along path-a while disordered SiO<sub>2</sub> film will be formed if the reactions go along path-b.

#### 4. Conclusions

The dissociative chemisorption reaction of TEOS on the substrate surface is the key step to understand SiO<sub>2</sub> film growth both in CVD and ALD processes. In this study, we reported the DFT first principles calculation results of TEOS surface reactions on fully hydroxylated SiO<sub>2</sub>(001) substrate. When performing the calculations, a model which breaking the reactions into two steps was proposed. Step one, one of the ethoxy functional groups of TEOS reacts with the surface OH and release an ethanol into the gas atmosphere. Our calculation result shows that the reaction of this step is thermodynamically favorable. Step two, another ethoxy functional group of the absorbed species (C<sub>2</sub>H<sub>5</sub>O)<sub>3</sub>Si continues to react with the nearby surface OH and release another ethanol. This will result in a stable adsorption with the formation of bridge like O–Si–O bonds. In this step, we studied the two potential reaction pathways and calculated their energy profiles. It was found that the pathway which will form crystal SiO<sub>2</sub> film is more energetically favorable than the one that will form disordered SiO<sub>2</sub> film. Our calculations suggested that with carefully choosing reaction conditions we can obtain conformal high quality SiO<sub>2</sub> film.

#### Acknowledgements

This study was financially supported by the National Science and Technology Major Project of China (2011ZX2403-002). Our work is completed on the “Explorer 100” cluster system of Tsinghua National Laboratory for Information Science and Technology.

#### References

- [1] K. Kamimura, D. Kobayashi, S. Okada, T. Mizuguchi, E. Ryu, R. Hayashibe, F. Nagaune, Y. Onuma, Preparation and characterization of SiO<sub>2</sub>/6h-sic

- metal-insulator-semiconductor structure using TEOS as source material, *Appl. Surf. Sci.* 184 (2001) 346–349.
- [2] N. Suzuki, K. Masu, K. Tsubouchi, Silicon dioxide film deposited by photoassisted microwave plasma cvd using teos, *Appl. Surf. Sci.* 79–80 (1994) 327–331.
- [3] S.M. George, A.W. Ott, J.W. Klaus, Surface chemistry for atomic layer growth, *J. Phys. Chem.* 100 (1996) 13121–13131.
- [4] M. Leskel, M. Ritala, Atomic layer deposition chemistry: recent developments and future challenges, *Angew. Chem. Int. Ed.* 42 (2003) 5548–5554.
- [5] T. Suntola, Atomic layer epitaxy, *Thin Solid Film* 216 (1992) 84–89.
- [6] J.D. Ferguson, E.R. Smith, A.W. Weimer, S.M. George, ALD of SiO<sub>2</sub> at room temperature using teos and H<sub>2</sub>O with NH<sub>3</sub> as the catalyst, *J. Electrochem. Soc.* 151 (2004) G528–G535.
- [7] M.E. Coltrin, P. Ho, H.K. Moffat, R.J. Buss, Chemical kinetics in chemical vapor deposition: growth of silicon dioxide from tetraethoxysilane (TEOS), *Thin Solid Film* 365 (2000) 251–263.
- [8] N. Sato, Y. Shimogaki, O<sub>3</sub>–TEOS CVD film formation on thermal SiO<sub>2</sub> pre-coated with ethanol, *ECS J. Solid State Sci. Technol.* 1 (2012) N73–N78.
- [9] N. Sato, Y. Shimogaki, Relationship between surface free energy of underlying layers and O<sub>3</sub>–TEOS chemical vapor deposition, *ECS J. Solid State Sci. Technol.* 2 (2013) N187–N190.
- [10] J.P. Perdew, J.A. Chevary, S.H. Vosko, K.A. Jackson, M.R. Pederson, D.J. Singh, C. Fiolhais, Atoms, molecules, solids, and surfaces: applications of the generalized gradient approximation for exchange and correlation, *Phys. Rev. B* 46 (1992) 6671–6687, PRB.
- [11] J.P. Perdew, J.A. Chevary, S.H. Vosko, K.A. Jackson, M.R. Pederson, D.J. Singh, C. Fiolhais, Erratum: Atoms, molecules, solids, and surfaces: applications of the generalized gradient approximation for exchange and correlation, *Phys. Rev. B* 48 (1993) 4978, PRB.
- [12] G. Kresse, J. Furthmüller, Efficiency of ab-initio total energy calculations for metals and semiconductors using a plane-wave basis set, *Comput. Mater. Sci.* 6 (1996) 15–50.
- [13] G. Kresse, J. Furthmüller, Efficient iterative schemes for ab initio total-energy calculations using a plane-wave basis set, *Phys. Rev. B* 54 (1996) 11169–11186.
- [14] D.J. Chadi, Special points for brillouin-zone integrations, *Phys. Rev. B* 16 (1977) 1746–1747.
- [15] G. Henkelman, H. Jónsson, Improved tangent estimate in the nudged elastic band method for finding minimum energy paths and saddle points, *J. Chem. Phys.* 113 (2000) 9978–9985.
- [16] G. Henkelman, B.P. Uberuaga, H. Jónsson, A climbing image nudged elastic band method for finding saddle points and minimum energy paths, *J. Chem. Phys.* 113 (2000) 9901–9904.
- [17] B. Han, Q. Zhang, J. Wu, B. Han, E.J. Karwacki, A. Derecskei, M. Xiao, X. Lei, M.L. O'Neill, H. Cheng, On the mechanisms of SiO<sub>2</sub> thin-film growth by the full atomic layer deposition process using bis(t-butylamino)silane on the hydroxylated SiO<sub>2</sub>(001) surface, *J. Phys. Chem. C* 116 (2011) 947–952.
- [18] J. Li, J. Wu, C. Zhou, B. Han, E.J. Karwacki, M. Xiao, X. Lei, H. Cheng, On the dissociative chemisorption of tris(dimethylamino)silane on hydroxylated SiO<sub>2</sub>(001) surface, *J. Phys. Chem. C* 113 (2009) 9731–9736.
- [19] B. Delley, An allelectron numerical method for solving the local density functional for polyatomic molecules, *J. Chem. Phys.* 92 (1990) 508–517.
- [20] B. Delley, From molecules to solids with the dmol3 approach, *J. Chem. Phys.* 113 (2000) 7756–7764.
- [21] W. Phadungsukanan, S. Shekar, R. Shirley, M. Sander, R.H. West, M. Kraft, First-principles thermochemistry for silicon species in the decomposition of tetraethoxysilane, *J. Phys. Chem. A* 113 (2009) 9041–9049.